Event-by-event fluid dynamcis

L. P. Csernai,[1,2] Zs. I. Lázár,[1,3] I. A. Lázár,[3] D. Molnár,[4] J. Pipek,[5] and D. D. Strottman[6]
[1]*Theoretical Physics Section, University of Bergen, Allegaten 55, 5007 Bergen, Norway*
[2]*KFKI Research Institute for Particle and Nuclear Physics, P.O. Box 49, 1525 Budapest, Hungary*
[3]*Department of Physics, Babeş-Bolyai University, M. Kogălniceanu 1, 3400 Cluj-Napoca, Romania*
[4]*Department of Physics, Columbia University, 538 West 120th Street, New York, New York 10027*
[5]*Department of Theoretical Physics, Technical University of Budapest, Budafoki út 8, H-1521 Budapest, Hungary*
[6]*LANSCE – DO, Los Alamos National Laboratory, Los Alamos, New Mexico 87545*
(Received 22 June 1999)

Coarse grained Langevin-type effective field equations may provide some guidance for the analysis of mesoscopic or microscopic molecular systems exhibiting fluctuations, or for systems of hundreds to thousands of atomic or subatomic particles produced in atomic or high-energy nuclear collisions. Suggestions for consistent realization of random fluctuations in discretized fluid dynamics will be presented.

PACS number(s): 05.40.−a, 47.11.+j

I. INTRODUCTION

Mesoscopic systems are of increasing importance, for example, in low-dimensional condensed matter or in high-energy nuclear collisions. The latter reactions provide a good application of the problem. Surviving macroscopic signals of quark-gluon plasma (QGP) formation such as entropy production and directed flow have been studied extensively. Critical fluctuations might also survive the subsequent dynamics [see the cosmic background explorer (COBE) experiments]. However, we need a well described prediction; otherwise we are just shooting randomly in the dark. Disoriented chiral condensate (DCC) fluctuations have been extensively discussed by now, but these should not be the only observable fluctuations we might be able to detect. Other quantities might also exhibit critical fluctuations. Different fluid-dynamical flow patterns are certainly candidates in which signs of critical fluctuations may be detected. For a more explicit example we have to study fluid dynamical fluctuations.

The size of a system where fluctuations become important is the order of the mean distance between the constituent particles, and the characteristic time of the dynamics of the system is comparable with the microscopic time scale. There are situations when the inclusion of fluctuations has a dramatic effect on the result. A good example is high-energy nuclear physics. As long as the matter of the expanding fireball is interacting, fluid dynamical or transport calculations can be applied, and they yield satisfactory explanations. On the other hand, fluid dynamical calculations or the solutions of kinetic models such as Boltzman-Uehling-Uhlenbeck (BUU), Vlasov-Uehling-Uhlenbeck (VUU), or Landau-Vlasov models cannot reproduce some fundamental features of the data. An example of such a feature is the fragment mass distribution. Averaging is done during the dynamics, and the resulting force fields are smooth. Therefore, no realistic clusterization is possible, and the only mass distribution emerging from such calculations is the one consistent with the law of mass action.

Unlike the above calculations, quantum molecular dynamical descriptions and solutions of Langevin-type dynamical equations do allow for more realistic clusterization. In both cases the averaging is done after the whole dynamics, meaning that the time evolution of all the elements of the ensemble occurs under the influence of fields that are different for each configuration. These fluctuating fields are responsible for the nontrivial fragment distributions.

Another phenomenon where fluctuations are crucial is sonoluminescence [1]. A micron-sized bubble in water driven by ultrasound can periodically collapse and revive, each time emitting one short blue flash coming from the bubble's very center. This light emission is due to extremely high temperatures (up to 10^5 K), which means a concentration of energy density by a factor of 10^{12}. Sonoluminescence has already gained applications in chemistry and medical physics, and some physicists have speculated about the possibility of achieving nuclear fusion. The sphericity of the collapse imposes the most serious limitation on the temperature, density, and size of the scorching central spot. The focusing mechanism can fail because of instabilities developing in both the liquid-gas interface and the surface of the converging shock wave. The instabilities are partly of microscopic origin, i.e., as time goes on, the shrinking shock surface ''senses'' more and more the effect of molecular fluctuations.

The goal of this work is to show how fluctuations can be consistently included into fluid dynamical equations. Since the problematics is complex, we shall use several simplifying assumptions. The range of applicability of the method described below is limited, but has all the essential ingredients emerging from the general considerations presented here, and allows for easy extension to more realistic problems.

II. FROM LANGEVIN EQUATION TO NAVIER-STOKES EQUATION

The inclusion of fluctuations into dynamical equations is not a new idea. Langevin's equation for the damped motion of a Brownian particle can be found in ordinary textbooks [2]. Certain aspects of fluctuations in fluid dynamics have been discussed as well [3].

The motion of a fluid is determined by the interaction

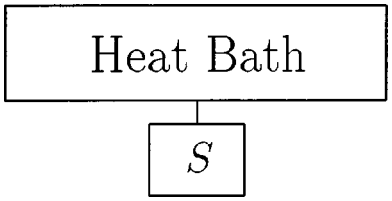

FIG. 1. A small system S interacting with an external heat bath with random thermal interaction forces. This is the case for the Brownian motion.

between its fluid elements. If these fluid elements are large but not macroscopic, the force they exert on each other can be separated into a smoothly varying average force and a fluctuating force due to the random thermal momentum transfer.

A. Langevin equation for external heat bath (Brownian motion)

Let us first take the simple example of Brownian motion. We can conceive it as the thermal interaction of a small system with an external heat bath (Fig. 1). There is a random momentum exchange F' between the system and the heat bath. Randomness does not exclude the presence of correlations. The dynamics of the Brownian particle is given by Langevin's equation

$$m[v(t+\tau)-v(t)]=\mathcal{F}(t)\tau-\alpha v(t)\tau+\int_t^{t+\tau}F'(s)ds, \tag{1}$$

where m and v are the mass and velocity of the Brownian particle. While $\mathcal{F}$ is an external force, F' fluctuates, satisfying the condition [2,4]

$$\langle F(s)\rangle_0=\langle F'(s)\rangle=0.$$

The averaging is done over the whole ensemble of the gas. α is a dissipative coefficient which is related to the ensemble average of the fluctuating force over the local thermal equilibrium ensemble

$$\alpha\equiv\frac{1}{2kT}\int_{-\infty}^{+\infty}\langle F(0)F(s)\rangle_0\,ds. \tag{2}$$

Equation (2) is the so-called *fluctuation dissipation theorem*. For Eq. (1) to apply, one has to stipulate that τ is larger than the relaxation time in the gas; that is, the collision time between the gas particles.

B. Langevin equation for internal heat bath

Let us imagine many small systems in contact with each other via both conservative forces and random momentum transfer (Fig. 2). Let us denote the random momentum received from $\boldsymbol{\mu}$ by element $\boldsymbol{\nu}$ as $\boldsymbol{p}_{\boldsymbol{\mu},\boldsymbol{\nu}}$ in a time interval between t and $t+\tau$. Due to the fact that we have an internal heat bath, where the subsystems are not negligibly small compared to each other, the random thermal momentum transfers are correlated:

$$\boldsymbol{p}_{\boldsymbol{\mu},\boldsymbol{\nu}}=-\boldsymbol{p}_{\boldsymbol{\nu},\boldsymbol{\mu}}.$$

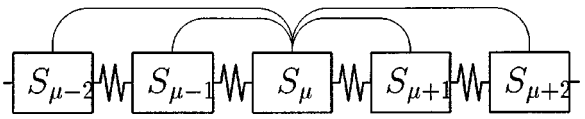

FIG. 2. A series of small systems, $S_{\mu-1}$, S_{μ}, $S_{\mu+1}$, ..., interacting with each other with random thermal momentum transfers (thin lines). The resulting random forces are classified into forces interacting with nearest neighbor volumes of about 1 m.f.p. distance from the fluid element in discussion $\boldsymbol{F}_{\mu}^{(1)}(t)$, with second nearest neighbor volumes of about 2 mean free path distance from the fluid element in discussion, $\boldsymbol{F}_{\mu}^{(2)}(t)$, ..., and so on. Furthermore, our small volume elements also interact with their nearest neighbors via nonrandom, harmonic forces (heavy lines).

This leads to a coupling among random forces in the medium. We can exploit this inversion symmetry with respect to the gridpoints, or fluid cells. The random force acting on a fluid cell labeled by $\boldsymbol{\mu}$ by its σth neighbors is

$$\boldsymbol{F}_{\boldsymbol{\mu}}^{(\sigma)}=\frac{\boldsymbol{p}_{\boldsymbol{\mu}-\boldsymbol{\sigma},\boldsymbol{\mu}}-\boldsymbol{p}_{\boldsymbol{\mu},\boldsymbol{\mu}+\boldsymbol{\sigma}}}{\tau}$$

and, so,

$$\boldsymbol{F}_{\boldsymbol{\mu}}=\sum_{\boldsymbol{\sigma}}\boldsymbol{F}_{\boldsymbol{\mu}}^{(\boldsymbol{\sigma})}, \tag{3}$$

where the sum $\Sigma_{\boldsymbol{\sigma}}$ runs over $\boldsymbol{\sigma}$ from σ_1, σ_2, $\sigma_3=1$ to ∞. Thus, exploiting the inversion symmetry, we constrain the summation to the positive quadrant of the $\boldsymbol{\sigma}$ space. If we know these random momentum exchanges for an ensemble, we can evaluate averages and correlation functions among them. The ensemble average of $\boldsymbol{F}_{\boldsymbol{\mu}}^{(\boldsymbol{\sigma})}$ for the actual ensemble of microstates does not vanish, $\langle\boldsymbol{F}_{\boldsymbol{\mu}}^{(\boldsymbol{\sigma})}\rangle\neq 0$, and it can be expressed via the correlation function of $\boldsymbol{F}_{\boldsymbol{\mu}}^{(\boldsymbol{\sigma})}$ taken over the equilibrium ensemble. This average force leads then to the viscous term in the ensemble-averaged equation of state.

We can replace summations over our fluid cells, labeled by $\boldsymbol{\sigma}$ or $\boldsymbol{\nu}$, by integrals over $\boldsymbol{y}$ or $\boldsymbol{r}$, where, e.g., $\boldsymbol{y}=\boldsymbol{\sigma}\Delta x_{\mathrm{cell}}$. After some calculation [5], in the continuum limit we find the Navier-Stokes equation with a fluctuating force density,

$$\frac{\partial\boldsymbol{M}}{\partial t}=-\boldsymbol{\nabla}(\boldsymbol{M}\circ\boldsymbol{v})-\boldsymbol{\nabla}P+\eta\nabla^2\boldsymbol{v}+\left(\zeta+\frac{1}{3}\eta\right)\boldsymbol{\nabla}(\boldsymbol{\nabla}\cdot\boldsymbol{v})+\boldsymbol{f}', \tag{4}$$

where $\boldsymbol{M}\equiv\rho\boldsymbol{v}$ is the momentum density and $(\mathbf{M}\circ\boldsymbol{v})_{ij}\equiv M_i v_j$. $\boldsymbol{f}'$ is the fluctuating part of the force density arising from random thermal interactions (so that for an ensemble of actual microstates $\langle\boldsymbol{f}'\rangle=0$), and the smooth part results in the dissipative viscous terms. In the limit of large subsystems $\boldsymbol{f}'$ vanishes not only for the ensemble average but also for every element of the ensemble. This shows that the inclusion of fluctuations for small subsystems is necessary, and its magnitude depends on the selected cell size. Thus, if we intend to discuss the fluctuations explicitly and quantitatively, we must use the discretized equations of fluid dynamics with well defined finite fluid cells. The magnitude of fluctuations will depend on the choice of size of the fluid cells, so the scale invariant feature of the fluid dynamics will

not hold. The cell size, consequently, should be chosen according to the physical problem.

Let us now see how fluctuations manifest themselves in the coarse-grained Navier-Stokes equation. After discretization, the right-hand side of Eq. (4) will be the sum of all forces acting on a certain fluid cell. The nonequilibrium part, $\boldsymbol{F}_{\boldsymbol{\mu}}^{\mathrm{ne}}$, of these forces can be separated into a dissipative term, $\boldsymbol{F}_{\boldsymbol{\mu}}^{\mathrm{diss}}$, and a purely fluctuating term, $\boldsymbol{F}_{\boldsymbol{\mu}}'$:

$$\boldsymbol{F}_{\boldsymbol{\mu}}^{\mathrm{ne}}=\boldsymbol{F}_{\boldsymbol{\mu}}^{\mathrm{diss}}+\boldsymbol{F}_{\boldsymbol{\mu}}',$$

where ''purely fluctuating'' means that $\langle \boldsymbol{F}_{\boldsymbol{\mu}}' \rangle = 0$ while the ensemble average of $\langle \boldsymbol{F}_{\boldsymbol{\mu}}^{\mathrm{diss}} \rangle$ gives the usual viscous terms [terms 3 and 4 in Eq. (4)]. Note that one of main assumptions in Ref. [5] when deriving Eq. (4) was that the fluctuations of the flow velocity $\boldsymbol{v}$ are small. This can be assured only if the fluctuating force, $\boldsymbol{F}_{\mu}'$, does not have too large amplitude either. From Ref. [5] [Eqs. (15) and (41)], we have for the dissipative term

$$\boldsymbol{F}_{\boldsymbol{\mu}}^{\mathrm{diss}}(t)=\frac{1}{kT}\int_{t}^{t+\delta t}\frac{dt'}{\delta t}\int_{0}^{\infty} ds \sum_{\boldsymbol{\nu}} \boldsymbol{Q}_{\boldsymbol{\mu\nu}}(s)\boldsymbol{v}_{\boldsymbol{\nu}}(t'-s), \quad (5)$$

where $\boldsymbol{Q}_{\boldsymbol{\mu\nu}}(s)\equiv\langle \boldsymbol{F}_{\boldsymbol{\mu}}(t)\circ\boldsymbol{F}_{\boldsymbol{\nu}}(t-s)\rangle_0$ is the correlation between forces acting on different cells at different times, and the summation runs over all the fluid cells. Naturally, this correlation depends only on the relative distance of the two cells. This form represents the fluctuation-dissipation theorem for the coarse-grained Navier-Stokes equation. The tensorial structure of $\boldsymbol{Q}_{\boldsymbol{\mu\nu}}(s)$ will yield both viscous terms in Eq. (4). In Appendix A we show that the continuum correspondent of $\boldsymbol{Q}_{\boldsymbol{\mu\nu}}(s)$ is the second time derivative of the momentum density correlation, C_{mom}^{D}, which can be connected with the second space derivative of the momentum current correlation C_{mom}^{C}. In one dimension this can be written as

$$Q(x,t)=\frac{\partial^2}{\partial t^2}C_{\mathrm{mom}}^{D}(x,t)=\frac{\partial^2}{\partial x^2}C_{\mathrm{mom}}^{C}(x,t),$$

where

$$C_{\mathrm{mom}}^{D}(x,t)\equiv\langle \delta M(y,s)\,\delta M(y-x,s-t)\rangle_0, \quad (6)$$

$$C_{\mathrm{mom}}^{C}(x,t)\equiv\langle \delta\Pi(y,s)\,\delta\Pi(y-x,s-t)\rangle_0,$$

are the density and current density correlation functions of the momentum, respectively. δM and $\delta\Pi$ are the density and current density deviations from the ensemble averages and the current density in its general multidimensional form is given by $\Pi_{ij}=M_i v_j+\delta_{ij}P+\sigma_{ij}$, where v_i is the flow velocity P the pressure and σ_{ij} is the dissipative stress tensor. At the moment we are not concerned with the complicated physics of the momentum current density, we just assume that it is known, and in practical applications we will have an ansatz for it. Since the first integral with respect to dt' in Eq. (5) is a simple averaging, it has no effect if δt is sufficiently small, and therefore can be omitted. The dissipative force density will be then

$$f^{\mathrm{diss}}(x,t)=\frac{1}{kT}\int_{0}^{\infty} ds \int_{-\infty}^{+\infty} dy \frac{\partial^2}{\partial y^2} C_{\mathrm{mom}}^{C}(x-y,s)\,v(y,t-s). \quad (7)$$

Note, that the integral form (7) exhibits advantages compared to the differential one in Eq. (4), provided that an ansatz for the momentum current correlation is available. In this way the instabilities can be handled in a viscous relativistic fluid dynamical approach. This formalism also enables us to present the dissipation fluctuation theorem in a consistent and transparent form. Assuming that the correlation function C_{mom}^{C} vanishes fast enough with distance, a double partial integration will yield

$$f^{\mathrm{diss}}(x,t)=\frac{1}{kT}\int_{0}^{\infty} ds \int_{-\infty}^{+\infty} dy\, C_{\mathrm{mom}}^{C}(x-y,s) \frac{\partial^2}{\partial y^2} v(y,t-s). \quad (8)$$

When the flow velocity field changes smoothly in time and space (near-equilibrium condition) the derivative of the velocity v can be taken outside the integral, and we are left with the usual viscous term in the one-dimensional correspondent of Eq. (4). Only the first dissipative term exists in this case, and the relation of the corresponding viscous coefficient to the equilibrium correlations is

$$\eta=\frac{1}{kT}\int_{0}^{\infty} ds \int_{-\infty}^{+\infty} dy\, C_{\mathrm{mom}}^{C}(x-y,s). \quad (9)$$

III. CONTINUUM FORMALISM

Landau and Lifshitz [3] approached the problem of hydrodynamical fluctuations. A rather concise, and from a formal point of view, simple formulation was presented for the fluctuation dissipation theorem. Using the published result, defining a fluctuating stress tensor s_{il}, we can write the correlation function of fluctuating force densities as

$$\begin{aligned}\langle f_i', f_l' \rangle &= \langle \partial_k s_{ik}(\boldsymbol{r},t)\,\partial_m s_{lm}(\boldsymbol{r}+\boldsymbol{y},t+s)\rangle \\ &= 2T\delta(s)\{\eta[\delta_{il}\nabla^2\delta(\boldsymbol{y})+\boldsymbol{\nabla}[\boldsymbol{\nabla}\delta(\boldsymbol{y})]\} \\ &\quad +(\zeta+\tfrac{1}{3}\eta)\boldsymbol{\nabla}[\boldsymbol{\nabla}\delta(\boldsymbol{y})]). \end{aligned} \quad (10)$$

One can see that integrating the equation of motion with a fluctuating force density [5], satisfying this correlation function, would yield the Navier-Stokes equation. The ''continuum limit'' of Eq. (5) would lead to the same tensorial form if we would go to zero with the correlation length by keeping the values of the correlations constant [5]. However, by going to the δ function limit, we lose the possibility of distinguishing between longitudinal and transverse correlation functions. Unfortunately, the usual choice of δ function for the shape of the correlation function leads to a vanishing fluctuation in this case even if we integrate this equation of motion over a locally equilibrated fluid cell. Thus for quantitative fluctuation studies, and to generate fluctuating forces for a discretized fluid dynamics this approach cannot be used.

The physical reason for this problem is that when making a ''continuum limit'' we should not go to zero with the cor-

relation length or mean free path, because we will tend to a perfect fluid. Then this very unphysical continuum limit cannot be easily reversed, and unfortunately the intermediate discretized model results are not given in the publication. Similar conclusions were found by Mansour *et al.* [6]. This result otherwise is equivalent to ours, and shows that the fluctuating force in fluid dynamics should have a complex tensorial structure.

IV. GENERATION OF FLUCTUATING TRANSPORTS FOR EXTERNAL HEAT BATH

A. Simplest case. Dirac delta correlation function

For a one-dimensional Brownian motion one can generate a force which has a fixed magnitude and random direction. It points either to the left or to the right. Obviously, such a fluctuation has a zero average. One can also fix the magnitude of the force from the fluctuation dissipation theorem [Eq. (2)], since the time correlation will be $\langle F'(0)F'(s)\rangle = |F'|^2\delta(s)$, yielding $|F'| = 2kT\alpha$. In conclusion, we gained a fluctuating force which, used in the Langevin equation, produced Brownian motion and was useful for studying certain aspects of the phenomenon. But while the damping of the velocity is described this way, correlation features of the fluctuations are lost.

B. Fluctuating force exhibiting time correlation

We can construct a more realistic approach by using a force acting on the Brownian particle. At a certain moment this force is determined by the state of the heat bath, which is in a causal relation with its foregoing states. Thus when generating the force we should be aware of at least two of its properties: stochastic character and memory. Let us discretize the time such that $f(t) = f(n\Delta t) \equiv f_n$, where $n = 0,1,2,\ldots,\infty$. A simple ansatz for the force could be

$$f_n = \xi_n f_{n-1} + (1-\xi_n) r_n ,$$

where ξ_n and r_n are uncorrelated random variables with values $\xi_n = \{0,1\}$, and $r_n = (-\infty, +\infty)$ and probabilities such that $P_\xi(0) \equiv 1 - \Delta t/\tau_{\rm coll}$, $P_\xi(1) = \Delta t/\tau_{\rm coll}$, $\langle r_n^{2m}\rangle = \text{const}$, $\langle r_n^{2m+1}\rangle = 0$, $n,m = 0,1,2,\ldots,\infty$. $\tau_{\rm coll}$ is the collision time of the molecules in the gas. Summarizing the results,

$$\langle f(t)\rangle = 0, \quad \langle f^{2m}(t)\rangle = \text{const}, \quad \langle f^{2m+1}(t)\rangle = 0,$$

$$K(t,s) = \langle f(t) f(t+s)\rangle = \langle f^2(t)\rangle e^{-s/\tau_{coll}},$$

$$K(t,s) = K(s) = K(-s).$$

Using this more realistic approach, all statistical moments of the fluctuation have the expected behavior, and also show a time correlation which exhibits the right properties.

V. GENERATION OF FLUCTUATING TRANSPORTS FOR INTERNAL HEAT BATH

The consistent generation of random transports for an internal heat bath is not as trivial as for Brownian particles, yet it is feasible. In this section we shall apply the ideas developed in the previous sections, and describe the steps necessary for the practical implementation of these ideas. The concrete task is to solve the discretized Navier-Stokes equation for an ideal gas with an extra random force term. We impose the following requirements.

(1) The extra term should have zero average.

(2) It should have a finite correlation time and length, the latter covering several numerical cells.

(3) The correlation function should satisfy the fluctuation-dissipation theorems (5) and (9).

(4) The conservation laws should not be violated by the fluctuations.

(5) The amplitude of the fluctuations should be relatively small in accordance with the assumptions made at the derivation of Eqs. (4) and (5). This also serves for avoiding nonlinearities arising from the fluctuations, i.e., the ensemble average of the solution should give back the result of plain calculation not including the fluctuating term $\boldsymbol{f}'$ in Eq. (4).

Presently, there are several methods to solve fluid dynamical problems. In this paper we shall concentrate on the inclusion of fluctuations into Eulerian numerical methods wherein the fluid is divided into cells by a fixed grid. The fluid is flowing through the walls separating the cells. For the sake of simplicity we only take a one-dimensional gas described by the flow variables $\rho(x,t)$, $M(x,t)$, and $E(x,t)$, denoting the mass, momentum, and energy densities at a given location and time. The set of coupled partial differential equations to be solved is

$$\frac{\partial \rho}{\partial t} + \frac{\partial \rho v}{\partial x} = 0, \tag{11}$$

$$\frac{\partial M}{\partial t} + \frac{\partial M v}{\partial x} = -\frac{\partial B}{\partial x} + f' \tag{12}$$

$$\frac{\partial E}{\partial t} + \frac{\partial E v}{\partial x} = -\frac{\partial B v}{\partial x}, \tag{13}$$

$$e = E - \frac{M^2}{2\rho}, \tag{14}$$

$$P = P(\rho, e), \tag{15}$$

where e is the thermal energy density. $B \equiv P + B^{\rm diss}$ yields the usual pressure P, and it has also a dissipative term $B^{\rm diss}$, depending on the flow velocity $v \equiv M/\rho$ in nonequilibrium situations. In most descriptions this term is similar to $B^{\rm diss} = \eta \partial v/\partial x$, where η is the viscous coefficient. The dissipative force [Eqs. (5) and (8)] is related to $B^{\rm diss}$ as $F^{\rm diss} = (\partial/\partial x) B^{\rm diss}$. Note that that fluctuation is included only in the momentum equation. No particle and heat diffusion is taken into account.

When discretizing Eqs. (11)–(15) we shall go back to the derivation of the Navier-Stokes equation from the internal heath-bath concept, and conceive the fluctuating force term as a result of random momentum transfers between cells. There are two possibilities: we can either generate uncorrelated transfers between all cells or correlated transfers between neighboring cells.

The first alternative is closer to the procedure of Sec II B, since the momentum arriving at a cell has the information about where it came from. This, together with proper retar-

dation effects, will yield the expected space-time correlations. It also has the advantage that the method allows for a relatively easy extension to more realistic modeling of random transports.

In the second case the information about the source of the incoming momentum is lost, and the correlations have to be enforced on the random transfers. On the other hand, this is also an advantage, since if one finds a good way of generating correlated random numbers the properties of the fluid can be effectively included in the random number generation. This approach maintains the general advantage of fluid-dynamical descriptions over molecular dynamical ones, insofar as only local information is needed for the solution. In this work we shall use the second alternative; that is, we shall generate space-time correlated random transports exclusively between neighboring cells.

A. Generation of a set of correlated random numbers

Our task is to generate an array (or grid) of random numbers, A_i, which all have a vanishing mean value and are correlated in the required way:

$$\langle A_\mu \rangle = 0, \quad \langle A_\mu A_\nu \rangle \equiv C_{|\mu-\nu|}, \tag{16}$$

i.e., the correlation of two elements in the array depends only on the ''distance'' between the two. One way to achieve our goal is to use auxiliary arrays. The main idea of the auxiliary array is the following: usually, the random number generators provide a sequence of uncorrelated numbers that are uniformly distributed within some interval. This can always be transformed so that the mean value will be zero and the distribution symmetrical about the origin. Let us denote these random numbers by R_μ. Formally, their properties can be written as

$$\langle R_\mu \rangle = 0, \quad \langle R_\mu R_\nu \rangle = \delta_{\mu\nu}. \tag{17}$$

This array of uncorrelated random numbers will be the auxiliary array. Schematically, our purpose is to find a linear transformation which creates the required array, A_μ, from R_μ:

$$R_\mu \xrightarrow[\text{linear transformation}]{} A_\mu. \tag{18}$$

Concretely, A_μ should be written as a weighted sum over the auxiliary grid, R_μ.

$$A_\mu = \sum_\nu c_\nu R_{\nu-\mu}, \tag{19}$$

where c_ν are a set of weights that depend on the desired shape of the correlation, $C_{|\sigma|}$. In order to see how this simple idea works, we shall resort to the continuum case. Let $R(\boldsymbol{y})$ be our continuum random function, which has a different (random) value at each point of the n-dimensional space. In accordance with Eq. (17)

$$\langle R(\boldsymbol{y}) \rangle = 0, \quad \langle R(\boldsymbol{x}) R(\boldsymbol{y}) \rangle = \delta(\boldsymbol{x}-\boldsymbol{y}). \tag{20}$$

This function is discontinuous at all points. Another discontinuous function $A(\boldsymbol{x})$ is written as

$$A(\boldsymbol{x}) \equiv \int d\boldsymbol{y} R(\boldsymbol{y}) c(\boldsymbol{y}-\boldsymbol{x}), \tag{21}$$

where the weight function $c(\boldsymbol{x})$ is a regularly behaving continuous function, and the integral is performed over the n-dimensional space of real numbers. Thus the average of $A(\boldsymbol{x})$ is zero, and its correlation function becomes

$$\langle A(\boldsymbol{x_1}) A(\boldsymbol{x_2}) \rangle = \int d\boldsymbol{y} c(\boldsymbol{y}) c(\boldsymbol{x_1}-\boldsymbol{x_2}+\boldsymbol{y}) \equiv C(\boldsymbol{x_1}-\boldsymbol{x_2}). \tag{22}$$

Obviously, $C(\boldsymbol{x})$ is also a continous regularly behaving function. Theoretically, our task is to find the weight function $c(\boldsymbol{x})$ from the desired correlation function $C(\boldsymbol{x})$ using Eq. (22). The general solution will not be discussed here, but note that this problem does not have a solution for an arbitrary $C(\boldsymbol{x})$.

Let us now restrict ourselves to the one-dimensional case, and take a Gaussian correlation function. We assume that a physical correlation extends to a distance λ, the correlation length. One can easily see that in order to obtain

$$C(x) = C_0 e^{-(x/\lambda)^2}, \tag{23}$$

we need to take a set of weights that also has Gaussian profile:

$$c(x) = \sqrt{\frac{2C_0}{\sqrt{\pi}\lambda}} e^{-2(x/\lambda)^2}. \tag{24}$$

We can verify easily that, by choosing $c_\mu = \sqrt{\Delta x} c(\mu \Delta x)$, the discretized version of Eq. (22) takes the form

$$C_{\mu-\nu} \equiv \langle A_\mu A_\nu \rangle = \sum_\sigma c_\sigma c_{\sigma+\mu-\nu}. \tag{25}$$

This is the discretized trapezoid approximation of integral (22) with an error, which is proportional to $(\Delta x)^2$.

B. Implementation of the correlated random array technique for conserved quantities

The simple Gaussian in Eq. (23) is not applicable as a correlation function of conserved densities, since these should obviously also show negative correlations. Moreover, having generated fluctuating densities in this way, their integral over the whole system will not stay constant but will fluctuate, though a lot less than for one cell. Such a method may respect conservation laws only on the average and not event by event, which is not satisfactory. These deficiencies are automatically remedied by using the above method for generating random currents instead of densities. Another strong argument for using random currents instead of densities is that, as shown at the end of Sec. II, in Eq. (7), it is sufficient to know the current correlation function C^C_{mom} to obtain the fluctuations and damping. One can show that if the fluctuating current of a conserved quantity shows correlation (23), the corresponding density correlations will also take negative values. More importantly, no matter what currents may occur among the cells, what is lost from one cell is

gained by another one; thus the total momentum will be conserved. Below we summarize all the simplifications used.

(1) The fluid is one dimensional, with an ideal gas equation of state $P=\rho c_s^2$, where P, ρ, and c_s are the pressure, mass density, and sound velocity, respectively.

(2) Random currents are considered between neighboring cells.

(3) Only momentum currents are generated randomly; particle and energy currents are neglected.

(4) Only spatial correlations are considered. Time correlations beyond one time step are neglected.

(5) All parameters entering the distribution function of the fluctuating term come from the equilibrium properties of the gas, assuming global equilibrium in our domain of computation. That is, we simulate an equilibrium fluctuation for the description of near-equilibrium processes (e.g., weak shock waves).

(6) The fluctuations are independent of the bulk dynamics, i.e., there is no feedback from the dynamics to the random transfers. This is reasonable as long as the relative amplitude of the fluctuations is small.

(7) The correlation length, λ correlation time τ, and other properties of the gas are considered as independent inputs, though they are connected by the relation $\lambda=v_T\tau$, where v_T is the thermal velocity of the gas.

(8) The method described here deals consistently with the first and second moments of the fluctuating quantities. Higher moments should not be studied with this method.

(9) The ansatz we used for the correlation function of the random momentum currents [Eq. (23)] is a simple Gaussian, but shows many of the essential features of a correlation function arising from kinetic theory.

There are three tasks: First, one should find an Eulerian fluid dynamical method to solve Eqs. (11)–(15) for the ''equilibrium'' case. Second, the dissipative nonequilibrium part of Eqs. (5) and (7) is included in the force term B in addition to the pressure. Third, the fluctuation is added to Eq. (12).

C. Inclusion of dissipation

One can see in Eq. (7) that the differentiation with respect to y can be changed to x, and taken outside the integral. Therefore, the nonequilibrium force term B^{diss} can be identified as

$$B^{\mathrm{diss}}(x,t)=\frac{1}{kT}\int_0^\infty ds\int_{-\infty}^{+\infty}dy\frac{\partial}{\partial y}C^C_{\mathrm{mom}}(x-y,s)v(y,t-s). \tag{26}$$

The ansatz for the correlation function can in principle be extended for time correlations as

$$C^C_{\mathrm{mom}}(x,t)=C_0e^{-(x/\lambda)^2-(t/\tau)^2}, \tag{27}$$

where λ and τ are direct inputs. The amplitude of the fluctuations, C_0, can be found by connecting the fluctuation-dissipation theorem (9) to elementary kinetic considerations. Performing the integrals in Eq. (9), and being aware that

$$\eta=\tfrac{1}{3}\rho v_T\lambda, \tag{28}$$

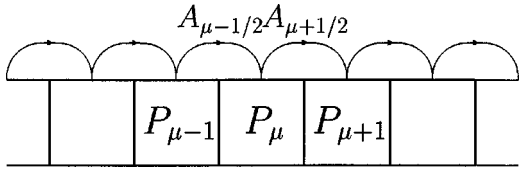

FIG. 3. The momentum P_μ of the fluid cell μ fluctuates because of the random momentum transfers $A_{\mu-1/2}$ and $A_{\mu+1/2}$ between neighboring cells.

where ρ is the density of the gas [2], we obtain

$$C_0=\frac{2}{3\pi}\frac{\rho v_T}{\tau}kT. \tag{29}$$

Once we have C_0 we have C^C_{mom}, and taking its derivative analytically, we can plug it into the kernel of the integral into Eq. (26). This can then be carried out numerically in the form of a sum over all fluid cells. When the system is considerably larger than the correlation length λ, the summation should be done only over those few cells that are close to the cell under consideration, and the Gaussian of the correlation function makes an important contribution. The discretized form of Eq. (26) will be

$$B^{\mathrm{diss}}_\mu(t)=\sum_{\nu=\mu-N_x/2}^{\mu+N_x/2}\sqrt{\pi}C_0\frac{\tau}{\lambda^2}(x_\mu-x_\nu)e^{-(x_\mu-x_\nu)^2/\lambda^2}v_\nu(t),$$

where N_x is the number of fluid cells where the correlation is cut off (see Appendix B). We used a numerical time step exceeding τ, so time correlations beyond one time step were neglected.

D. Inclusion of fluctuations

In this work we considered near-equilibrium fluctuations conceived as equilibrium fluctuations superimposed on near-equilibrium dynamics. Therefore, fluctuations were handled independently from the bulk dynamics of the fluid. The time sequence of the necessary steps is the following.

(1) Calculate the dissipative force term B^{diss} as it was described in Sec. V C, and plug it into the fluid dynamical equations (12) and (13).

(2) Proceed with the solution of Eqs. (11)–(15) one time step.

(3) Add to the momentum of each cell a random value generated as described below.

(4) Start again from (1).

The random value added to the momentum P_μ of a cell at position μ is calculated as the difference of two currents $A_{\mu-1/2}$ and $A_{\mu+1/2}$, entering the left side and leaving through the right side, respectively. Naturally, the outgoing current on the right will be the ingoing one for the cell's right neighbor at $\mu+1$ (see Fig. 3). The change of the momentum, ΔP_μ, will be

$$\Delta P_\mu=A_{\mu-1/2}-A_{\mu+1/2},$$

where the correlated array of random transfers $A_{\mu+1/2}$ is generated as described in Sec. V A. The easiest way of handling the boundaries is to consider the gas inside a large box,

closed at both ends, and then no special considerations should be given to cells next to the boundaries. There will be a random momentum flow through the boundaries as well, since momentum is not conserved in this case. However, if one also includes random energy or mass transfers between the cells, which is not done in this work, their flow through the boundaries should be set to zero in order to maintain the energy and mass of the fluid constant.

VI. APPLICATION FOR WEAK SHOCKS

As an illustration we will study the effect of fluctuations and dissipation on weak shocks. The advantage of shocks, for example, is in the dependence of the shock front width on viscosity. The front width and viscous coefficient show a linear interdependence [7]. The weakness of the shock is necessary for satisfying the near-equilibrium requirement, which was a basic assumption in the derivation of Eq. (5). In addition, the description of shocks exhibits an acute need for consistent inclusion of dissipation which has a dominant role in the study of flow discontinuities. For the outcome of certain fluid dynamical phenomena, the width and structure of shock fronts is of great relevance. A good example is sonoluminescence. The self-collision of a converging spherical shock yields infinite temperature and pressure in the very center of the bubble if the shock front is modeled as a sharp discontinuity (Sec. II, Chap. XII, of Ref. [7]). However, if viscosity is included and the shock front has a finite width, the central temperature becomes finite as well, but its amplitude continuously being hypersensitive to the shock width [8]. The gradients are enormous and the number of particles involved in the light emission are only of the order of 10^6.

Unfortunately, in numerical hydrodynamical codes viscosity is not easy to control. This is partially due to the presence of *numerical viscosity* inherent to all numerical methods. It increases with increasing numerical cell size Δx, and the width of shock fronts is proportional to it. We will use Δx as length unit in our calculations presented in the examples below. Including dissipative terms in the equation of motion, while decreasing the cell size to a level where the numerical viscosity is negligible compared to the physical one, may yield other problems, such as instabilities arising from the derivatives in the viscous terms. Therefore, in many cases numerical viscosity is advantageous.

In our example we consider a one-dimensional ideal gas enclosed in a box and moving with a relatively low velocity v_0 to the right. A weak shock propagates in the opposite direction. Formally $v_0/c_s \ll 1$, where v_0 is the velocity with which the gas hits the right wall and c_s the sound velocity in the noncompressed gas. $(\rho_1-\rho_0)/\rho_0 \ll 1$, where ρ_0 and ρ_1 are the densities of the noncompressed and compressed gas, respectively. If we ignore the fluctuations and zoom in the shock front region, we obtain a set of density profiles for different correlation lengths (Fig. 4). This means increasing viscosity in accordance with Eq. (28). Note that since there is no fluctuation included, by correlation length we mean the distance within which the integrand in Eq. (9) is not negligible. The solid line with the steepest slope corresponds to a zero viscosity parameter. The effect of numerical viscosity is remarkable if we compare this profile with the dashed one. The latter one represents the exact perfect fluid dynamical solution by a step function. Such a solution could in principle be obtained by decreasing the cell size below any limit. As the correlation length λ increases, more and more cells are involved in the calculation of the dissipative term (5). Therefore, the smoother and smoother shock profiles correspond to increasing physical viscosities. Including fluctuations should not cause a deviation of the ensemble average from the nonfluctuating profiles, as shown in Fig. 5. However, Fig. 6 shows easily noticeable deviations of the mean values from the nonfluctuating solutions in Fig. 4. It reports significant nonlinearities arising because of the finite amplitude of the fluctuations.

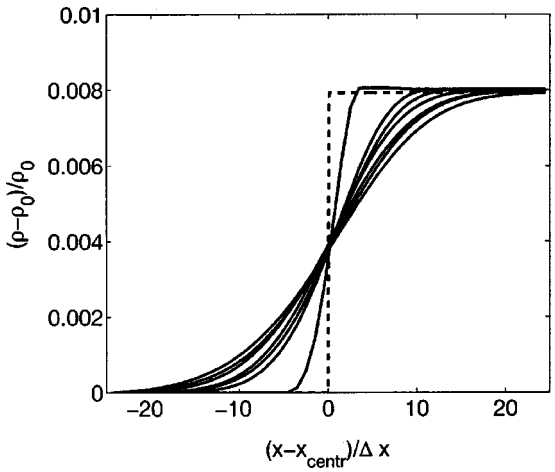

FIG. 4. Increase of the local density in shock front profiles for different correlation lengths, λ, i.e., different viscosities, η [Eq. (28)]. On the horizontal axis the numbers label the numerical fluid cells included in the window delimiting the front region studied. The dashed line corresponds to the perfect fluid solution, $\eta=0$. This is not a result of a fluid dynamical calculation but a simple step function. The solid curves represent numerical results. The steepest front corresponds to $\eta=0$, manifesting numerical viscosity, while the rest corresponds to increasing correlation lengths, $\lambda = 0.6, \ldots, 3.6\Delta x$. The number of cells involved in the summation in the dissipative term (5) is cut off at 1, 2, 4, 5, 7, 8, and 10 (see Appendix B).

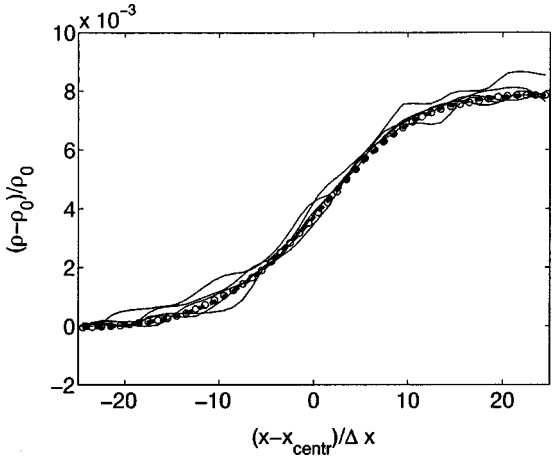

FIG. 5. The ensemble average of fluctuating hydrodynamical calculations of a shock. The thin lines are members of the ensemble, the circles are the average of the ensemble, and the thick dashed line is the nonfluctuating profile.

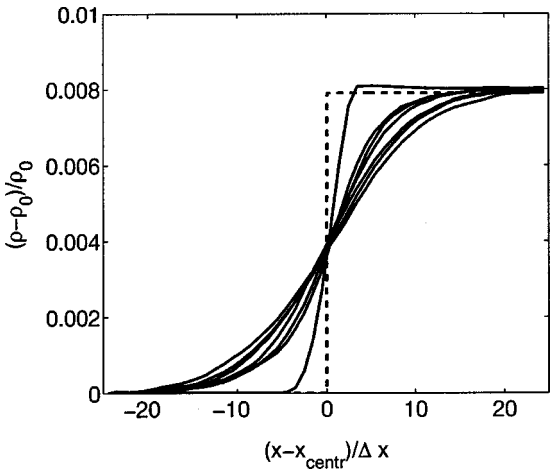

FIG. 6. Same as Fig. 4, with fluctuations included. The solid lines represent the ensemble averages. Slight deviations from Fig. 4 are due to nonlinearities arising because of the finite amplitude of the fluctuations.

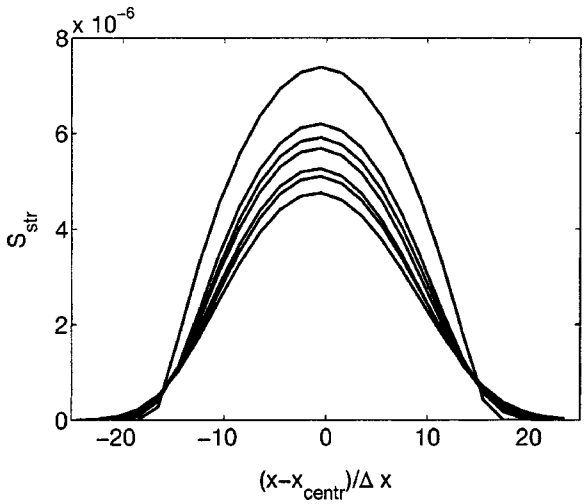

FIG. 7. Dependence of the structural entropy S_{str} on the position of the front relative to the window (see Fig. 4). x_{centr} is the position of the center of the shock. The maximum of structural entropy is obtained when the front is in the middle of the window. Different curves correspond to the different viscosities (top→largest).

Structural entropy as tool for studying shock front profiles

In order to have a more quantitative description of what we can see in Figs. 4 and 6, we shall use the concept of structural entropy employed in the study of superstructures in extended systems [9]. Following the notation from this reference, let us consider a normalized, positive definite distribution Q_i over a one-dimensional lattice of N cells:

$$\sum_{i=1}^{N} Q_i = 1, \quad Q_i \geqslant 0.$$

We can introduce the so called delocalization measure D, defined as

$$D \equiv \left[\sum_{i=1}^{N} (Q_i)^2 \right]^{-1}, \tag{30}$$

and the well-known Shannon entropy S, defined as

$$S \equiv -\sum_{i=1}^{N} Q_i \ln Q_i . \tag{31}$$

The definition of the structural entropy is

$$S_{\mathrm{str}} \equiv S - \ln D. \tag{32}$$

The study of different shapes of the distribution, Q_i, in the (r, S_{str}) diagram, where $r \equiv -\ln D/N$, has important advantages. One remarkable feature of the structural entropy is that, unlike the Shannon entropy, it does not diverge as the cell size goes to zero. Practically, it is independent of the discretization of the distribution.

For the study of the shock front shape, we fixed a ''window'' on the x axis of a given width which was roughly of the size of the largest expected front width, and studied the evolution of the density profile. Note that the structural entropy S_{str} of a step-function-like shock front is sensitive to the location of the front with respect to the window.

Figure 7 shows the structural entropy as a function of time (or position of the front) as the front passes through the window. The different curves stand for the different viscosities. S_{str} is zero as long as the front is outside the window, and has a maximum around the middle. Generally, the position of the maximum for a step function strongly depends on the ratio of the maximum and minimum for that function. However, in our case the weakness of the shock makes the maximum deviate negligibly from the midpoint of the window. We shall compare the shapes of the different fronts at this point because here the error, due to a possible slight shift between the fronts, will be minimal. Figures 4 and 6 are also ''pictures'' taken through the above mentioned window, at the moment when S_{str} is at maximum.

As we can see in Fig. 8, the higher the viscosity and smoother the profile, the more S_{str} approaches the origin in the (S_{str}, r) diagram. The rightmost point (a) corresponds to the ideal nonviscous shock front, described by a step function, while the second (b) shows the effect of numerical viscosity in our calculation for a given grid size Δx. Beyond that, starting from (c), we can see the effect of physical viscosity which dominates the numerical one.

With the help of Fig. 9, we can estimate the value of the numerical viscosity. As in Fig. 8, point (a) corresponds to zero physical viscosity, while (c) and further points stand for increasing physical viscosities which dominate the numerical one. We fit the calculated points with a curve that emerged from density profiles approximated by the function

$$\rho(x) = \rho_0 + \frac{\rho_{\max} - \rho_0}{2} \{ \tanh[\alpha \eta^q (x - x_{\mathrm{centr}})] + 1 \}, \tag{33}$$

where we used the values $\alpha = 0.18$ and $q = -0.4$. α is given in units of $(\rho k T \Delta x/3)^{-q}/\Delta x$. Numerical calculations with this method and gridsize should be used in cases when the structural entropy $S_{\mathrm{str}} \ll 7.4 \times 10^{-6}$ at point (b) in Fig. 9. This means that such numerical calculations involve a numerical viscosity which can be estimated based on the fitted curve as $\eta_{\mathrm{num}} \approx 0.1 \rho v_T \Delta x/3$. Only problems with viscosity exceeding η_{num} should be handled with this method. Here, as we only

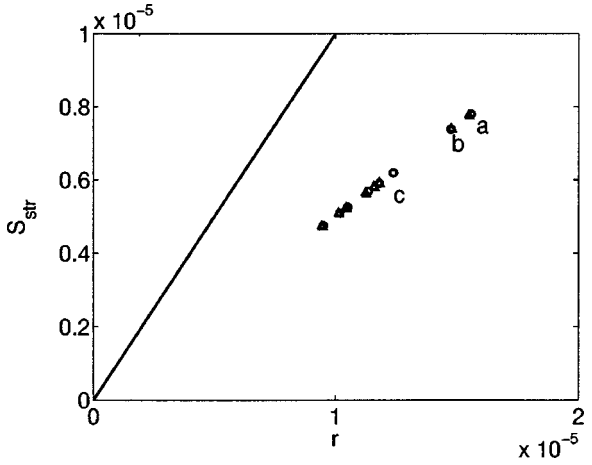

FIG. 8. Structural entropy $S_{\rm str}$ vs r [Eq. (32)] for the shock front profiles in Figs. 4 and 6. The discretized distribution in Eqs. (30) and (31) is $Q_i \equiv \rho_i / \Sigma_k \rho_k$, where ρ_i is the density at the ith cell and the summation is done over cells within the window containing the shock front profiles. The circles stand for the nonfluctuating calculations (Fig. 4), and the triangles for ensemble averages including the fluctuations (Fig. 6). The first point (a) corresponds to zero physical and zero numerical viscosity. Points at (b) represent zero physical and finite numerical viscosity. Starting from (c), physical viscosity dominates. No points can exist above the solid line (see Ref. [9]).

provided a few points, the exact determination of $\eta_{\rm num}$ is not feasible, but the principle can also be used with more precise calculations.

VII. SUMMARY

The method presented here provides us with an ensemble of fluid dynamical solutions, where fluctuations are included. While fluctuations are averaged out within each fluid cell, the fluctuations among the cells are taken into account. This is an important improvement in the description of mesoscopic and/or very dynamical systems for two reasons: (i) fluctuations and their consequences can be described realistically, and (ii) viscous effects are treated more realistically via the fluctuation-dissipation theorem. Physically this is apparent in cluster formations and surface instabilities. Also, it will be possible to study mesoscopic correlations, together with the corrections these effects cause for collective fluid dynamical observables.

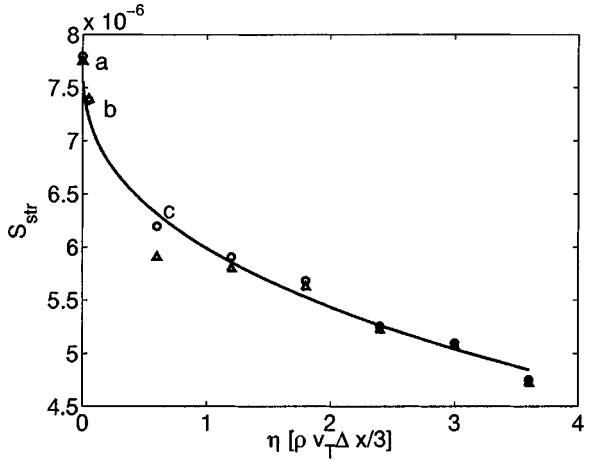

FIG. 9. Structural entropy $S_{\rm str}$ vs the viscosity. For a perfect fluid [point (a)], i.e., $\lambda = 0$ and $\eta = 0$, the step function yields $S_{\rm str} = 7.8 \times 10^{-6}$. The numerical viscosity with the same η and λ parameters [point (b)] yields fronts of finite width and structural entropy of $S_{\rm str} = 7.4 \times 10^{-6}$. $\eta_{\rm num} \approx 0.1 \rho v_T \Delta x/3$ is the approximate value of the numerical viscosity that can be inferred from the fit [Eq. (33)] along the physical viscosity points. (c) and further points represent physical viscosities (see Fig. 8).

APPENDIX A: DENSITY AND CURRENT DENSITY CORRELATION RELATIONS

Let us consider the scalar density of some conserved quantity, ρ, and its corresponding three-dimensional current density vector, j_i, $i = 1$, 2, and 3. Imagine that for some reason they fluctuate without violating the conservation law. Their mean values are $\langle \rho \rangle$ and $\langle j_i \rangle$, and their deviations from the means are $\delta\rho$ and δj, respectively. The continuity equation should hold:

$$\frac{\partial \rho}{\partial t} + \nabla_i j_i = 0. \tag{A1}$$

Taking the ensemble average of Eq. (A1), we find the same equation for the mean values. After subtracting the latter from Eq. (A1) we again obtain a similar equation for the deviations:

$$\frac{\partial}{\partial t} \delta\rho + \nabla_i \delta j_i = 0.$$

Therefore, it is true that

$$\frac{\partial^2}{\partial t_1 \partial t_2} C^D(\boldsymbol{r_1} - \boldsymbol{r_2}, t_1 - t_2) = \nabla_{1i} \nabla_{2j} C^C_{ij}(\boldsymbol{r_1} - \boldsymbol{r_2}, t_1 - t_2), \tag{A2}$$

where $C^D(\boldsymbol{r_1} - \boldsymbol{r_2}, t_1 - t_2) \equiv \langle \delta\rho(\boldsymbol{r_1}, t_1) \delta\rho(\boldsymbol{r_2}, t_2) \rangle$ and $C^C_{ij}(\boldsymbol{r_1} - \boldsymbol{r_2}, t_1 - t_2) \equiv \langle \delta j_i(\boldsymbol{r_1}, t_1) \delta j_j(\boldsymbol{r_2}, t_2) \rangle$ are the autocorrelation functions of the deviations at different points and times. They depend only on the relative positions and time difference. Consequently, Eq. (A2) can be written as

$$\frac{\partial^2}{\partial t^2} C^D(\boldsymbol{r}, t) = \nabla_i \nabla_j C^C_{ij}(\boldsymbol{r}, t). \tag{A3}$$

In one dimension Eq. (A3) reduces to

$$\frac{\partial^2}{\partial t^2} C^D(x, t) = \frac{\partial^2}{\partial x^2} C^C(x, t).$$

The generalization for nonscalar densities is trivial.

APPENDIX B: DETAILS OF THE NUMERICAL CALCULATION

We use a one-dimensional SHASTA algorithm [10] for propagating the flow variables ρ, M, and E [Eqs. (11)–(15)] [Sec. V B, item (1)]. The correlated random momentum transfers are generated according to Sec. V A, for all times at

the very beginning of the calculation [Sec. V B, items (5) and (6)]. In our case this is possible because we discuss weak shocks, so that global equilibrium is a good approximation to predict thermal fluctuations. SHASTA and the momentum transfers are performed successively in each time step. Below, we indicate the parameters necessary to reproduce our results. Since we only studied the shock front through a narrow window, the actual number of numerical cells for the whole fluid is irrelevant. It can be anything as long as it is lot more than the maximum number of cells involved in the front profile and the front is far enough from the boundary of the fluid. An important parameter of the SHASTA algorithm is $v\Delta t/\Delta x$, a quantity which must be less than 1/2 in order to assure that the conservation laws hold. Here v is the flow velocity, and Δt and Δx are the time step and cellsize, respectively. In this work the length scale is given in terms of Δx in concrete examples. Since in our case the shock is very weak, the maximum velocity is equal to the sound velocity, c_s, which is chosen to be $c_s=0.21\Delta x/\Delta t$ in our calculation, presented as an example. Similarly, the other parameters are $v_0/c_s=1/85$, $\tau=0.035\Delta t$, and $\Delta N=11000$, where v_0 is the initial velocity of the gas at which it runs into a wall somewhere at the right, τ is the correlation time, and ΔN is the number of particles in one cell. The correlation length of the fluctuations, λ, was varied (and as a consequence η was also varied), taking values of $\lambda=0.6,\ldots,3.6\Delta x$. One may choose Δx and Δt and the mass of a particle, m, to be suitable for the particular problem studied. From the following relations one can find the rest of the quantities, $\rho=m\Delta N/\Delta x$ and $C_0=2/3\pi\rho/mc_s^2/\tau$, where C_0 is the amplitude parameter in the correlation function [Eqs. (27) and (29)]. Note that we assumed that the thermal velocity v_T equals the sound velocity c_s.

We also assumed that the spatial correlation function is cut off at a number of cells, N_x, given by the condition $\exp(-(N_x\Delta x/\lambda)^2)<10^{-3}$. This is meant to include those and only those cells where the correlation function makes a significant contribution to integral (9). In addition, the random array technique presented in Sec. V A can produce undesired effects if the weight function $c(x)$ in Eq. (24) is not allowed to decrease sufficiently.

ACKNOWLEDGMENTS

One of the authors (J.P.) wishes to thank the Országos Tudományos Kutatási Alap (OTKA) (Grant No. T024136) for financial support and Professor L. P. Csernai for kind hospitality.

[1] L. A. Crum, Phys. Today **47** (9), 22 (1994).

[2] F. Reif, *Fundamentals of Statistical and Thermal Physics* (McGraw-Hill, New York, 1965).

[3] L. D. Landau and E. M. Lifshitz, Zh. Éksp. Teor. Fiz **32**, 618 (1957) [Sov. Phys. JETP **5**, 512 (1957)]. The authors thank Tamás Tél of L. Eötvös University, Budapest for drawing their attention to this publication.

[4] R. Balescu, *Equilibrium and Nonequilibrium Statistical Mechanics* (Wiley, New York, 1975).

[5] L. P. Csernai, S. Jeon, and J. I. Kapusta, Phys. Rev. E **56**, 6668 (1997).

[6] M. M. Mansour, A. L. Garcia, G. C. Lie, and E. Clementi, Phys. Rev. Lett. **58**, 874 (1987); A. L. Garcia, M. M. Mansour, G. C. Lie, M. Mareschal, and E. Clementi, Phys. Rev. A **36**, 4348 (1987); A. L. Garcia, M. M. Mansour, G. C. Lie, and E. Clementi, J. Stat. Phys. **47**, 209 (1987); F. Baras, M. M. Mansour, and A. L. Garcia, Am. J. Phys. **64**, 1488 (1996).

[7] Ya. B. Zel'dovich and Yu. P. Raizer, *Physics of Shock Waves and High-Temperature Hydrodynamic Phenomena* (Academic, New York, 1966).

[8] C. C. Wu and P. H. Roberts, Phys. Rev. Lett. **70**, 3424 (1993); W. C. Moss, D. B. Clarke, J. W. White, and D. A. Young, Phys. Fluids **6**, 2979 (1994).

[9] J. Pipek and I. Varga, Phys. Rev. A **46**, 3148 (1992).

[10] J. P. Boris and D. L. Book, J. Comput. Phys. **11**, 38 (1973); D. L. Book, J. P. Boris, and K. Hain, *ibid.* **18**, 248 (1975); J. P. Boris and D. L. Book, *ibid.* **20**, 397 (1976).